ISPRS Journal of Photogrammetry and Remote Sensing 81 (2013) 1–11

Contents lists available at SciVerse ScienceDirect

ISPRS Journal of Photogrammetry and Remote Sensing

journal homepage: www.elsevier.com/locate/isprsjprs

# Development of a 3-D urbanization index using digital terrain models for surface urban heat island effects

Chih-Da Wu [a], Shih-Chun Candice Lung [a,b,*], Jihn-Fa Jan [c]

[a] Research Center for Environmental Changes, Academia Sinica, Taipei, Taiwan
[b] Department of Atmospheric Sciences, National Taiwan University, Taipei, Taiwan
[c] Department of Land Economics, National Chengchi University, Taipei, Taiwan

ARTICLE INFO

*Article history:*
Received 8 January 2013
Received in revised form 5 March 2013
Accepted 22 March 2013
Available online 30 April 2013

*Keywords:*
Surface urban heat island (SUHI)
Heat wave
Medium-sized city
Three-dimension urbanization index
Urban climate

ABSTRACT

This study assesses surface urban heat island (SUHI) effects during heat waves in subtropical areas. Two cities in northern Taiwan, Taipei metropolis and its adjacent medium-sized city, Yilan, were selected for this empirical study. Daytime and night time surface temperature and SUHI intensity of both cities in five heat wave cases were obtained from MODIS Land-Surface Temperature (LST) and compared. In order to assess SUHI in finer spatial scale, an innovated three-dimensional Urbanization Index (3DUI) with a 5-m spatial resolution was developed to quantify urbanization from a 3-D perspective using Digital Terrain Models (DTMs). The correlation between 3DUI and surface temperatures were also assessed. The results obtained showed that the highest SUHI intensity in daytime was 10.2 °C in Taipei and 7.5 °C in Yilan. The SUHI intensity was also higher than that in non-heat-wave days (about 5 °C) in Taipei. The difference in SUHI intensity of both cities could be as small as only 1.0 °C, suggesting that SUHI intensity was enhanced in both large and medium-sized cities during heat waves. Moreover, the surface temperatures of rural areas in Taipei and Yilan were elevated in the intense heat wave cases, suggesting that the SUHI may reach a plateau when the heat waves get stronger and last longer. In addition, the correlation coefficient between 3DUI and surface temperature was greater than 0.6. The innovative 3DUI can be employed to assess the spatial variation of temperatures and SUHI intensity in much finer spatial resolutions than measurements obtained from remote sensing and weather stations. In summary, the empirical results demonstrated intensified SUHI in large and medium-sized cities in subtropical areas during heat waves which could result in heat stress risks of residents. The innovative 3DUI can be employed to identify vulnerable areas in fine spatial resolutions for formulation of heat wave adaptation strategies.


## 1. Introduction

As global warming continues to raise the average temperature of our planet, heat waves have become more frequent with record-breaking temperatures (Solomon et al., 2007). These high temperatures and the increasing number of heat-related deaths worldwide over the last decade have demonstrated the significant impacts of extreme temperature on human health (Confalonieri et al., 2007; Tan et al., 2010). On top of global warming, urban heat island (UHI) effect aggravates the temperature increase in urban areas (Smoyer-Tomic et al., 2003). UHI effect is the result of urbanization which involves concentrated energy consumption and dense urban infrastructures. Numerous previous studies have examined the UHI in large cities, which are defined as a metropolitan area identified as an area has a population of one million or more (United State Census Bureau, 2013). For example, UHI was assessed as 5 °C in Birmingham (second most populous city), UK, 7 °C in London, UK, and Shanghai, China, 8 °C in New York City, US, and Seoul, Korea, 10 °C in Beijing, China, and 12 °C in Tokyo, Japan (Watkins et al., 2002; Gedzelman et al., 2003; Hung et al., 2006; Tomlinson et al., 2012). As the world population continuously moves to urban areas (United Nations, 2008), the numbers of medium-sized cities account for the majority (UNICEF, 2012). Thus, it is important to assess the UHI effects not only in metropolitans but also in medium-sized cities. The definitions of a medium-sized city are varied (Kunzmann, 2009). The most common definition is that of a town with a population of 20,000 up to 200,000 (Rondinelli, 1993). Several studies have examined UHI at the medium-sized cities in European countries (Alonso et al., 2003; Unger et al., 2011; Papanastasiou and Kittas, 2012). Less often considered are the non-mega cities of Asia.

* Corresponding author. Address: 128, Section 2, Academia Road, Nangang, Academia Sinica, Taipei 115, Taiwan. Tel.: +886 2 2653 9885x277; fax: +886 2 2783 3584.
*E-mail address:* sclung@rcec.sinica.edu.tw (Shih-Chun Candice Lung).

0924-2716/$ - see front matter © 2013 International Society for Photogrammetry and Remote Sensing, Inc. (ISPRS) Published by Elsevier B.V. All rights reserved.
http://dx.doi.org/10.1016/j.isprsjprs.2013.03.009

Warm extremes of temperature have adverse effects on health (Gosling et al., 2007). Different 'threshold temperature' have been identified for a variety of causes of death (Huynen et al., 2001; Páldy et al., 2005). Comparative studies have shown the occurrence of geographical variation in 'threshold temperature'. Heat-related mortality thresholds occur at higher temperatures in locations with a relatively warmer climate, and the gradient (or steepness) of the temperature-mortality relationship for increasing temperature is often found to be lower in warmer locations than colder ones (Donaldson et al., 2003; Pattenden et al., 2003). For example, Kalkstein and Davis (1989) estimated a threshold for Dallas at 40 °C; Dessai (2002) obtained a threshold of 29 °C for Lisbon. Thresholds may be confounded by other meteorological variables, e.g. Saez et al. (2000) illustrated a 2 °C higher threshold (23 °C) on very humid days when the relative humidity was above 85% in Barcelona, Spain, but there is also evidence that humidity may have insignificant effects on mortality (Braga et al., 2001; Dessai, 2003). The variation of thresholds and temperature-mortality gradients has led to inference on how populations may acclimatize to changing climatic conditions (Donaldson et al., 2003; Gosling et al., 2007).

Surface temperature is of prime importance to the study of urban climate in understanding the environmental conditions necessary for human beings (Hung et al., 2006). In contrast to the direct in situ measurements made of atmospheric heat islands, thermal remote sensors observe the surface urban heat island (SUHI) based on the spatial patterns of upwelling thermal radiance received by the remote sensors (Oke et al., 1991; Voogt and Oke, 2003). Currently, advanced remote sensing techniques enable us to examine the long-term SUHI effects and urban climates of a large spatial area (Streutker, 2003; Weng et al., 2004). Previous research has mostly studied the SUHI effects on megacities in the temperate climate zone without considering the influence of heat waves (Gallo and Owen, 1998; Bottyán et al., 2005; Hung et al., 2006). No study investigates the SUHI effects under extreme heat conditions in the subtropical climate zone.

The two dominant human elements affecting the development of UHI effects are population and built-up factors (Oke, 1982; Arnfield, 2003; Yow, 2007). Among built-up factors, built-up ratio and spatial pattern of land-use types have been well defined in previous studies (Zha et al., 2003; Matinfar et al., 2007) while fewer studies considered building height and building volume in UHI assessment (Oke, 1973; Bottyán et al., 2005). Accurate estimation of building heights across an extensive area poses tough challenges. To take such a challenge, this work develops a new three-demensional (3-D) urbanization index (3DUI) considering both vertical and horizontal built-up configurations with fine spatial resolution using high resolution digital terrain models (DTMs). This index, as seen in the subsequent results, allows scientists to study temperature variability and UHI intensity at 5-m spatial resolution, which can be used to identify vulnerable areas in formulating heat wave adaptation strategies.

This study focused on utilizing remote sensing and Geographic Information System (GIS) to investigate SUHI during heat waves in the northern Taiwan based on several selected heat wave cases, which can be viewed as a model example with Asian characteristics such as dense population distribution and intense land utilization. The objectives of this work are (1) to evaluate the SUHI intensity during heat waves in two subtropical cities with case studies; (2) to quantify the surface temperature during heat waves in Yilan area, a medium-sized city, compared to Taipei metropolis, a large city; and (3) to develop a new 3-D urbanization index for examining the urban development, which can be used to study the distribution of surface temperature and SUHI intensity at 5-m spatial resolution.

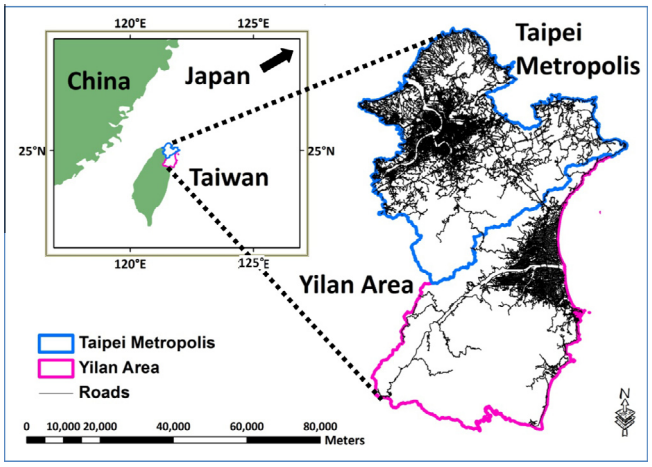


**Fig. 1.** Location of the study area.

## 2. Materials and methods

### 2.1. Study area and database

Two locations in the northern Taiwan were selected, namely Taipei metropolis (a large city) and its adjacent Yilan area (a medium-sized city, Fig. 1). Taipei metropolis consists of Taipei city (the capital of Taiwan) and New Taipei city. It covers 2324.4 $km^2$ and includes 41 towns. More than 1/4 of the population in Taiwan lives in this area, approximately 6.5 million with a density of 2791 people/$km^2$ (DGB, 2011). Based on the national land use inventory (NLSMC), 13.20% of the Taipei metropolis is impermeable surface (e.g., building and roads) and 68.33% is covered by forest (NLSMC, 2009). The Yilan area covers 2143.6 $km^2$ and includes 12 towns surrounded by agricultural areas and forest. Compared with Taipei metropolis, Yilan, though with a similar area, has a smaller population size (0.46 million) and a much lower population density (213 people/$km^2$). Compared with Taipei metropolis, less impermeable surface (3.83%) but more forest (75.76%) is found in Yilan (NLSMC, 2009).

Five datasets were used in this study. They were (1) the national land-use inventory, (2) Digital Terrain Models (DTMs), (3) Taiwan's socio-economic classification of urban development, (4) weather records from the Central Weather Bureau (CWB), and (5) Land-Surface Temperature (LST) data from Moderate Resolution Imaging Spectroradiometer (MODIS). The national land-use inventory and DTMs were used for the establishment of 3DUI which is described in Section 2.2.2. The national land-use inventory generated using 1/5000 scale aerial photos collected from 2006 to 2008 was acquired (NLSMC, 2009). Land-use type including constructions for transportation, recreation, public and private buildings were selected as the human constructions for establishing the 3DUI. In addition, DTMs with 5-m spatial resolution processed from aerial photos taken during 2004–2005 were also employed to establish the 3DUI. DTMs provide a mathematical representation of topography (Alagarni and El Hassan, 2001) and are classified into two categories, Digital Elevation Model (DEM) and Digital Surface Model (DSM). DEM consists of terrain elevations for natural ground surfaces at regularly spaced horizontal intervals (USGS, 2011). While DSM not only incorporates natural ground surfaces, but also takes into account buildings and other objects higher than the underlying topographic surfaces, such as trees and rooftops (Brunn and Weidner, 1998). The horizontal and vertical variations of DEM

and DSM in urban locations are less than 0.5 m and 0.7 m, respectively (SSC, 2011).

Daily air temperature records of the Central Weather Bureau (CWB) stations in Taipei and Yilan from 2000 to 2010 were used to identify heat wave events and select heat wave cases. There is no universal definition of a heat wave (Meehl and Tebaldi, 2004). According to Wu et al. (2010b), 35 °C and 32 °C of the daily maximum temperature were used as the cut-off points for selecting heat wave cases in Taipei and Yilan areas, respectively. Moreover, with reference to the traditional Chinese Farmers' Almanac, which has been used for over two thousand years, days near July 21 are the hottest period throughout the whole year, and it is usually true nowadays according to CWB records. Therefore, we adopted July 21 as a reference day. Around July 21, a period of excessively hot weather lasting more than 10 days was identified as a heat wave event. The day with the maximum daily temperature during the heat wave event was selected as the studied case. Five cases were chosen, including July 23, 2000, July 22, 2002, July 21, 2004, July 22, 2007, and July 3, 2010. Furthermore, cases in 2004, 2007, and 2010 were specified as intense heat wave cases because the duration of extremely high temperatures of the three cases was longer than 2 weeks in both Taipei metropolis and Yialn area. Table 1 list the selected dates of the five heat wave cases and the metrological observations obtained from the CWB stations of Taipei and Yilan.

The MODIS/Terra Version 5 LST Global 1 km Grid products are produced daily using the generalized split-window LST algorithm, which was validated by field campaigns and radiance-based validation studies and ready for use in science applications (Wan, 2009). The unit of LST products is Kelvin (K). The valid range of the pixel values is from 7500 to 65,535. The value of pixels was then multiplied by a scale factor of 0.02 to obtain the thermodynamic temperature (K). In this study, we have transferred the unit of LST maps from thermodynamic temperature (K) to Celsius temperature (°C). The Terra MODIS instrument acquires data twice daily (10:30 am and 10:30 pm in Taiwan). In Taiwan, it is not easy to acquire cloud free images in summer time because of the typical subtropical weather type with frequent afternoon clouds and thunderstorms. Besides, shadow effects are also common due to a mountainous terrain (Wu et al., 2010a). Therefore, LST maps with more than 65% of the cloud-free pixels in the study area were adopted as the study materials. Based on the criteria, images of two selected cases (night time on July 22 and daytime on daytime on July 3, 2010) were too cloudy to use; thus, the dates with the second highest daily maximum temperature with available satellite images were used instead. Differences of the daily maximum temperatures between the original and alternative dates for the two cases were smaller than 0.9 °C. Moreover, to avoid the cloud effects on the surface temperature observations, only pixels which were cloud-free in all the five cases were kept in the database for further analyses. The effects of topographic shading on LST were neglected in this study since relatively lower elevation relief was found in the two selected locations of our study (109 and 351 m for urban and rural areas in Taipei, 108 and 592 m for urban and rural areas in Yilan, respectively), based on estimation method from Liu et al. (2006). Finally, 10 selected LST maps (five in daytime and five in night time) from the U.S. Geological Survey (USGS) data archive were used in this study. In these adopted LST images, 41% of the study area was cloud-free (total 1204 $km^2$) and were used for our analysis. Fig. 2 shows the daytime and night time LST maps used in this study.

Urban and rural areas in Taipei and Yilan were identified according to Taiwan's socio-economic classification of urban development based on population density and economic development index with the resolution of townships (Hou et al., 2008). The average elevations for urban and rural areas are 109 and 351 m in Taipei and 108 and 592 m in Yilan, respectively. A decrease of about 0.6 °C/100 m is employed to correct the adiabatic lapse rate (Courault and Monestiez, 1999). A correction coefficient ($C_t$) was added to the estimated temperatures of rural areas according to their difference in elevation with urban areas. In this study, $C_t$ is 1.4 for Taipei metropolis and 2.9 for Yilan area, respectively.

## 2.2. Data processing and methods

### 2.2.1. Calculation of SUHI intensity

SUHI intensity is calculated as the difference between the spatial mean temperatures of urban and mean rural over the study area obtained from LST maps. Such computations provide a more robust measure of SUHI intensity and minimize the inherent variability between observing sites that can impact the magnitude of SUHI values (Streutker, 2003; Weng et al., 2004). SUHI intensity was calculated for Taipei metropolis and Yilan area for the five heat wave cases in order to assess their intensity during heat waves. It should be noted that the difference in vegetation cover between 2002 and 2007 was less than 0.5% in both Taipei and Yilan (Forest Bureau, Republic of China, 2012). Therefore, the difference in change of land cover during the study periods should not affect our comparison results and can be ignored.

### 2.2.2. Development of 3DUI

3DUI is a quantitative 3-D urbanization index, which takes into account the total volume of human constructions of an area, including building and transportation constructions. Compared with the other 2-D urbanization indices (e. g. ratio of impervious surface), 3DUI provides a quantitative measurement of urbanization from a 3-D perspective. 3-D urbanization characteristics can be effectively obtained from the 3DUI using GIS and DTMs with a 5-m spatial resolution. The heights of human constructions were calculated by subtracting the elevation values in DEM from those in DSM for the man-made land-use types in the national land-use inventory. Road pavements are also important anthropogenic constructions in a city. However, the thickness (height) of roads is generally assumed as zero in DTMs. Since man-made road surfaces can absorb heat, affect surface temperatures, and contribute to SUHI intensity, a constant of 0.2 m was adopted as the thickness of roads according to the "Regulations of Urban Road Designs" (Ministry of the Interior, Republic of China, 2011). The results were then multiplied by the size of pixel (5 m × 5 m = 25 $m^2$) to derive the total volume of human constructions. The calculation of 3DUI is as follow.

$$3DUI_i = (Hdsm_i - Hdem_i) \times A_i \quad (1)$$

where $3DUI_i$ ($m^3$/pixel) is the 3-D Urbanization Index of pixel $i$, $Hdsm_i$ (m) and $Hdem_i$ (m) denote the elevation recorded in DSM and DEM of pixel $i$, respectively, and $A_i$ ($m^2$) is the size of pixel $i$ (5 m × 5 m = 25 $m^2$). There is no upper limit for 3DUI while the lower limit is 0. A large 3DUI indicates intense human development or constructions in the area. As for the pixels with natural land covers (i.e. forest, water, and crops), their values are assigned as "0" because there was no human construction in these areas.

3DUI of both Taipei metropolis and Yilan area were established. In order to evaluate whether 3DUI is a good indicator for assessing surface temperature variability and SUHI, the correlations of 3DUI values and surface temperature from LST for each heat wave case were assessed with Spearman's rank correlation. The results are presented and discussed in the following section.

**Table 1**
Five selected cases and their meteorological observations at Taipei and Yilan weather stations.

| | Taipei metropolis | | | Yilan area | | |
|---|---|---|---|---|---|---|
| | Maximum temperature (°C) (daytime) | Minimum temperature (°C) (night time) | Consecutive days | Maximum temperature (°C) (daytime) | Minimum temperature (°C) (night time) | Consecutive days |
| Case 1 23-July-2000 | 35.6 | 25.8 | 10 | 33.9 | 24.9 | 16 |
| Case 2 22-July-2002 | 35.1 | 25.5 | 12 | 32.0 | 23.7 | 13 |
| Case 3 21-July-2004 | 35.1 | 27.1 | 14 | 32.8 | 25.1 | 26 |
| Case 4 22-July-2007 | 38.0 | 28.2[a] | 16 | 34.3 | 26.9[a] | 31 |
| Case 5 3-July-2010 | 37.7[b] | 27.8 | 14 | 33.5[b] | 25.9 | 23 |

[a] Temperature of July 21 was listed instead because the cloud cover in the satellite image of night time on July 22, 2007 exceeded 35%.
[b] Temperature of July 5 was listed instead because the cloud cover in the satellite images of daytime on July 3 and 4, 2010 exceeded 35%.

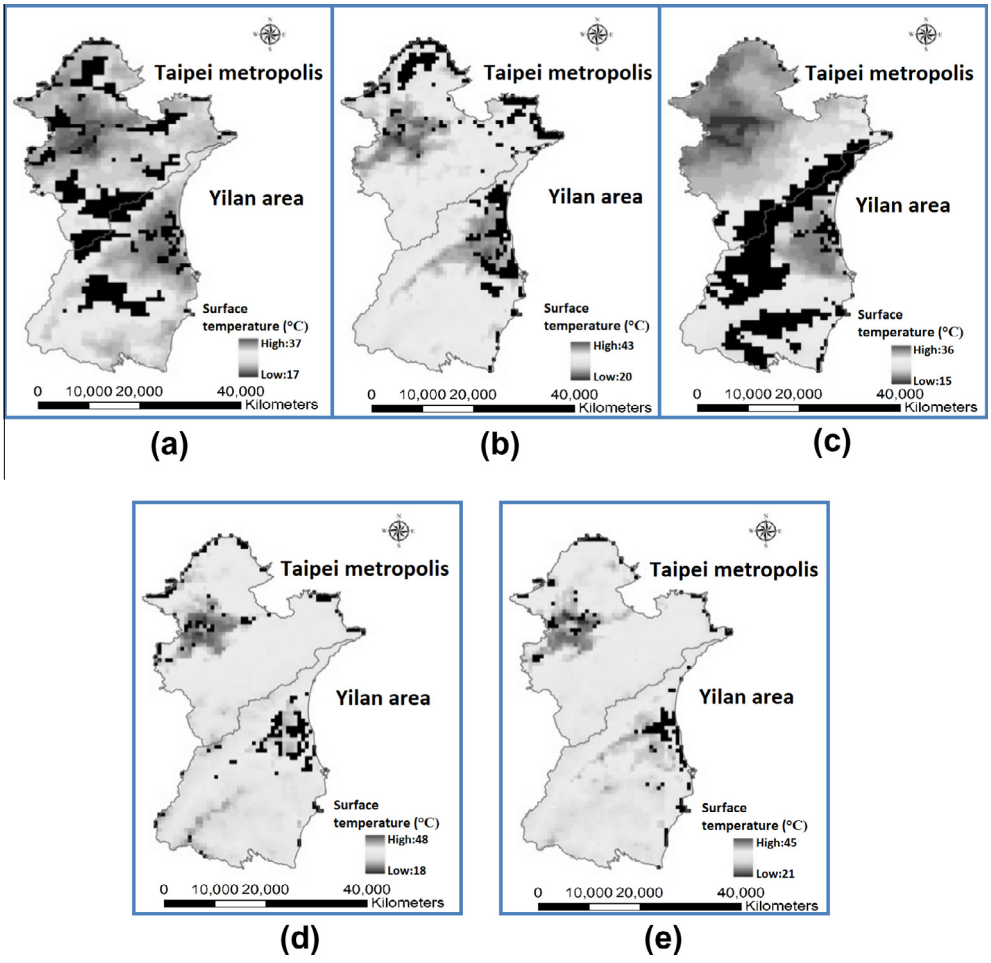


**Fig. 2.** Daytime and Night time LST maps used in this study. From (a–e) show the daytime maps of July 22, 2000, July 22, 2002, July 21, 2004, July 22, 2007, and July 3, 2010, respectively. (f–j) are the Night time maps of July 22, 2000, July 22, 2002, July 21, 2004, July 21, 2007, and July 5, 2010, respectively. Grey in the maps indicates high surface temperature while white represents cool condition. Black indicates the cloud areas.

## 3. Results and discussion

### 3.1. Surface temperature of different urbanization types

Table 2 shows the average surface temperatures of urban and rural areas in Taipei metropolis and Yilan. In these two cities, urban areas usually displayed the warmest signals at both daytime and night time, while rural areas were always the coolest in the five cases as expected. The highest daytime temperature was 43.8 °C and 37.2 °C in urban Taipei and Yilan, respectively; both occurring on July 22, 2007 (case 4).

Liao (2008) found high correlation (correlation coefficient = 0.832) between MODIS LST and air temperature measurements of 123 CWB stations in Taiwan. This finding demonstrated that, although LST and air temperature are not directly comparable, however, in the case of UHI, it is reasonable to believe that spatial trends will be similar when comparing LST and air temperature (Tomlinson et al., 2012). Therefore, the aforementioned air and surface temperatures from our study imply that residents in urban areas of both Taipei and Yilan are at risks of heat stress during the heat waves.

For the intense heat wave cases in both Taipei and Yilan, temperatures remained high during night time in both urban and rural areas. As mentioned, air and surface temperatures show similar trend in temporal variation. Therefore, such continuously elevated temperatures would increase physiological burden, leading to increased morbidity and mortality, particularly among the elderly (WHO, 2009). In Taipei and Yilan, seniors aged above 65 years account for 10% (approximate 0.64 million) and 13% (approximate 0.03 million) of the population, respectively (Ministry of the Interior, Republic of China, 2012a). These vulnerable groups are potentially at risk of heat stress due to the synergic impact of SUHI effects and heat waves.

Comparison between the two cities reveals that the temperature observed in Taipei metropolis was always higher than that in Yilan area. The temperature differences between Taipei and Yilan were the largest in urban areas most of the time for both daytime and night time. The largest difference (6.6 °C) occurred during daytime of July 22, 2007. The surface temperature of urban areas in Taipei even exceeded 40 °C in the cases of 2007 and 2010. Such high temperatures in urban areas were the result of synergic effects of SUHI and heat waves. In terms of air temperatures of Taipei and Yilan (Table 1), which represents temperature measurements on the observational sites with the standard metrological instruments, the maximum daily temperatures in urban Taipei exceeded 35 °C while those at urban Yilan exceeded 32 °C in 2007 and 2010. Wu et al. (2010b) indicated that significant mortality (21.0 per 100,000 people) was observed in Taiwan at such high air temperatures. Our study demonstrates that attention should be paid to vulnerable groups in both large and medium-sized cities during heat waves. Moreover, diurnal temperature range (DTR) is a risk factor of mortality independent of the corresponding temperature (Kan et al., 2007). However, previous studies assessed the association of DTR and health outcomes in winter time and no study examines the impacts of DTR changes on health effects in summer time, especially during heat waves. Therefore, more studies should be conducted to assess this issue further.

### 3.2. SUHI intensity during heat waves

#### 3.2.1. SUHI intensity of Taipei metropolis

Figs. 3a and 4a illustrate the daytime and night time SUHI intensity, respectively, of Taipei metropolis of the five selected heat wave cases. The SUHI intensity in daytime could reach 10.2 °C in Taipei, while the largest SUHI intensity in night time was 4.3 °C. The largest SUHI intensity in daytime occurred in the intense heat wave case of 2007 while that in night time occurred in the intense heat wave case of 2004. It shall be noted that not all SUHI intensity in the intense heat wave cases were higher than those in the non-intense heat wave cases. The reason for lower SUHI intensity during intensive heat wave is increase in rural temperatures rather than decrease in urban temperatures. During the intense cases of 2004, 2007, and 2010 in Taipei (Figs. 3a and 4a), not only the urban temperatures stayed high but also the rural temperatures elevated in both daytime and night time.

Liao (2008) used MODIS data to investigate the SUHI of four major cities in Taiwan during 2003–2005. Totally, 50 MODIS images in non-heat wave days were applied to assess the seasonality of surface temperature and SUHI. Their results showed that the SUHI intensity in summer was 4.7 °C in daytime and 1.7 °C in night time, respectively, which were lower than those of the five heat wave cases assessed in this work (Figs. 3 and 4). These results suggest that SUHI intensity on the heat wave days in Taipei may be stronger than that on non-heat-wave days.

Furthermore, these results were compared with SUHI intensity observed in other Asian and western cities. Hung et al. (2006) used remote sensing for comparative assessment of SUHI in mega cities of Asia. Their results found that, in August 2001, Tokyo had the highest daytime SUHI intensity of 12 °C, followed by Beijing (10 °C), Seoul (8 °C), Shanghai (7 °C) and Pyongyang (4 °C); Stathopoulou and Cartalis (2007) showed that the SUHI intensity of Athens, the most urbanized city of Greece, was 3.3 °C; Pongracz et al. (2006) indicated that the most intense SUHI effect (around 4 °C) of the ten most populated cities of Hungary, occurred during daytime, in the summer season. Compared with these studies, our results showed that Taipei had similar SUHI intensity (9.9 °C in Case 2 and 10.2 °C in Case 4) with Beijing.

#### 3.2.2. SUHI intensity of Yilan area

Similar to the Taipei metropolis, Yilan area also showed higher SUHI intensity in daytime (Figs. 3b and 4b). Again, Fig. 3 showed that the Yilan area had lower daytime SUHI intensity in the intense heat wave cases (2004, 2007, and 2010) compared with the other two cases. Rural temperature was elevated (up to 33 °C in 2004) in the three intense heat wave cases, thus narrowing the urban–rural temperature differences. The elevated temperature also occurred in the night time cases of 2007 and 2010. The stomata closure at high temperatures may be the major reason for the increase in rural temperature during intense heat wave. Of the Yilan area, 75.8% is covered with vegetation or forest (NLSMC, 2009). Seasonal and evergreen vegetations normally have high moisture availability contributing to evapotranspiration for cooling down the ambient temperature. The behavior of stomata is the major mechanism for controlling the evapotranspiration and release of water vapor from plants. As leaf temperature increases above the optimum, the intercellular $CO_2$ concentration would increase, resulting in stomata closure to prevent the loss of water content (Meidner and Heath, 1959; Sheriff, 1979; Schroeder et al., 2001). During intense heat waves, this stomata closure mechanism may slow down the ambient temperature regulation by vegetation, leading to increase in surface temperature of rural areas. During the 2003 European heat waves, regional impacts of $CO_2$ emissions from plants rather than $CO_2$ uptakes were observed due to stomata closure of vegetation under the extreme summer heat (Ciais et al., 2005); thus, it is possible that stomata closure mechanism is also the major reason for the observed temperature elevation in night time in this work. More investigations are needed to improve our understanding on the physical causes of the increase of rural temperature during heat waves. Nevertheless, the reduction of SUHI intensity in Yilan during the intense heat wave cases was observed compared with the other two cases. These results suggest that the

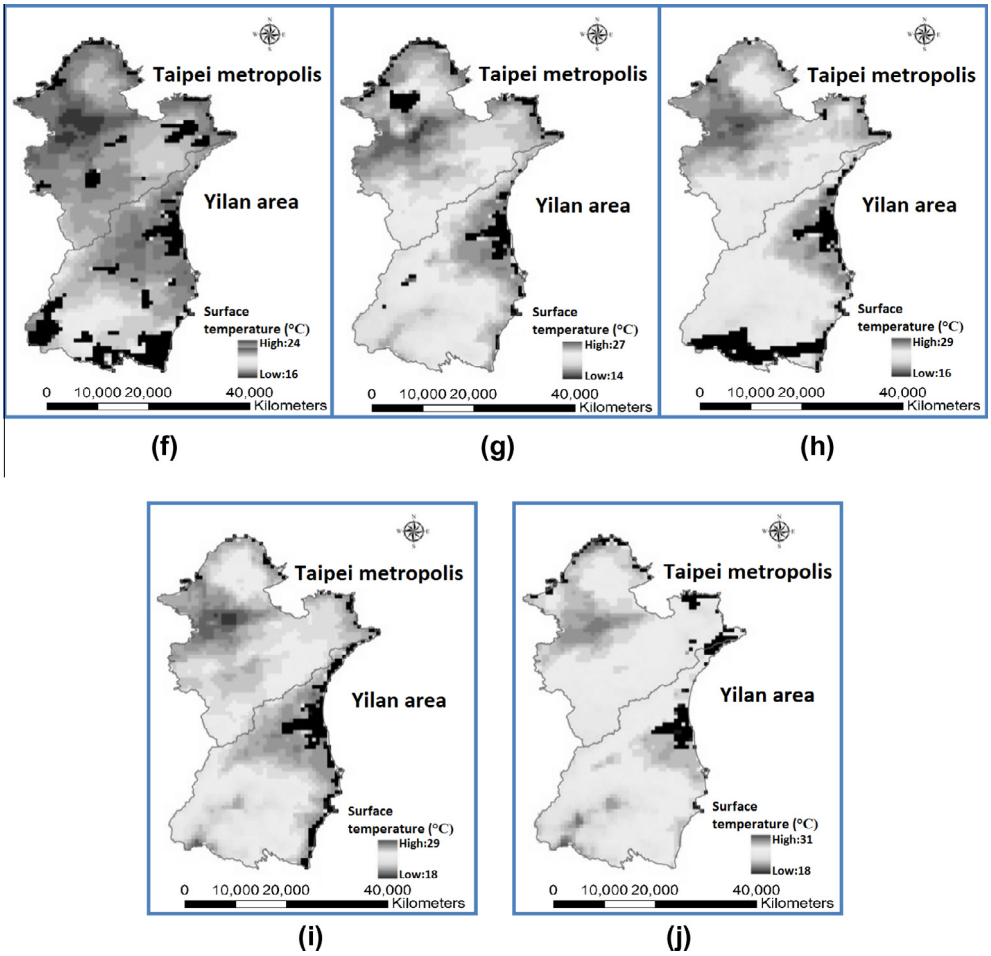


**Fig. 2.** (*continued*)

**Table 2**
Average surface temperature (°C) of urban and rural areas from MODIS LST data.

| | Urban type | Daytime | | | Night time | | |
|---|---|---|---|---|---|---|---|
| | | Taipei | Yilan | Difference | Taipei | Yilan | Difference |
| Case 1 | Urban | 35.2 | 33.4 | 1.8 | 23.4 | 21.4 | 2 |
| -2000 | Rural area | 28.3 | 27.5 | 0.8 | 21.4 | 21.6 | −0.2 |
| Case 2 | Urban | 39.4 | 37 | 2.4 | 25.2 | 24 | 1.2 |
| -2002 | Rural area | 29.6 | 29.5 | 0.1 | 22.9 | 21.5 | 1.4 |
| Case 3 | Urban | 39.6 | 35.9 | 3.7 | 27.1 | 24.9 | 2.2 |
| -2004 | Rural area | 33 | 33.7 | −0.7 | 22.8 | 21.3 | 1.5 |
| Case 4 | Urban | 43.8 | 37.2 | 6.6 | 27.3 | 25.8 | 1.5 |
| -2007 | Rural area | 33.6 | 32.5 | 1.1 | 24.7 | 24.7 | 0 |
| Case 5 | Urban | 40.2 | 36.8 | 3.4 | 27.5 | 25.6 | 1.9 |
| -2010 | Rural area | 33.4 | 32.4 | 1.0 | 24.1 | 25 | −0.9 |

SUHI may reach a plateau when the heat waves get stronger and last longer.

### 3.2.3. Comparison of SUHI intensity between Taipei and Yilan

Comparing the two cities revealed that Taipei consistently had greater SUHI intensity than Yilan. The maximum difference of 5.5 °C was observed in the daytime case of 2007. Nevertheless, the difference can be as small as only 1.0 °C (case 1 in 2000, daytime). The results demonstrate that, a medium-sized city like Yilan also experienced significant SUHI intensity of up to 7.5 °C. It should be noted that satellite images obtained at 10:30 am in Taiwan may not capture the largest SUHI intensity in Taipei and Yilan, which is expected to occur between noon and 2 pm. In other words, it is highly likely that the SUHI intensity goes beyond the temperature of 10.2 °C and 7.5 °C in Taipei and Yilan, respectively, as presented in this work.

## 3.3. 3-D urbanization index

### 3.3.1. Description of 3DUI results

3DUI was developed to quantify the urbanization from a 3-D perspective with 5-m spatial resolution data. The building heights

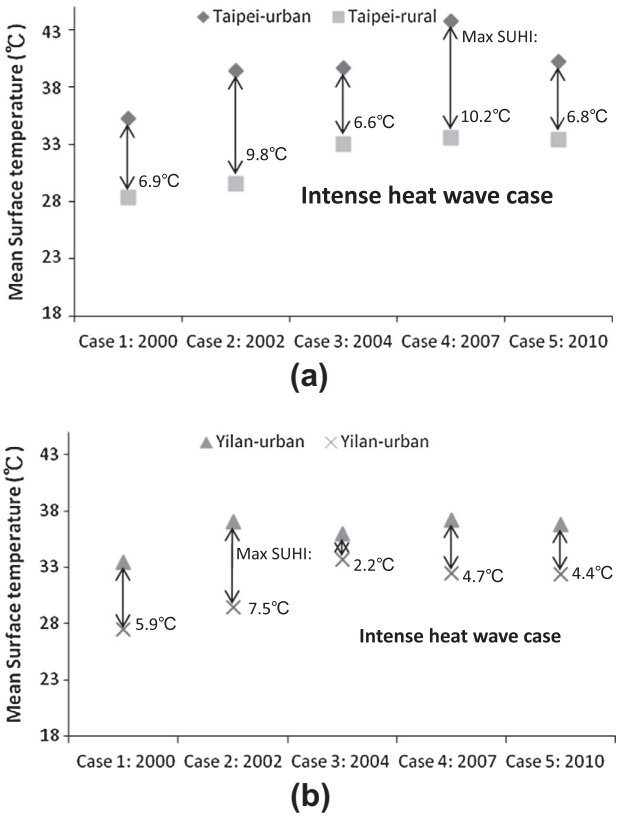


**Fig. 3.** Daytime SUHI intensity (°C) of (a) Taipei metropolis and (b) Yilan area of the five selected heat wave cases.

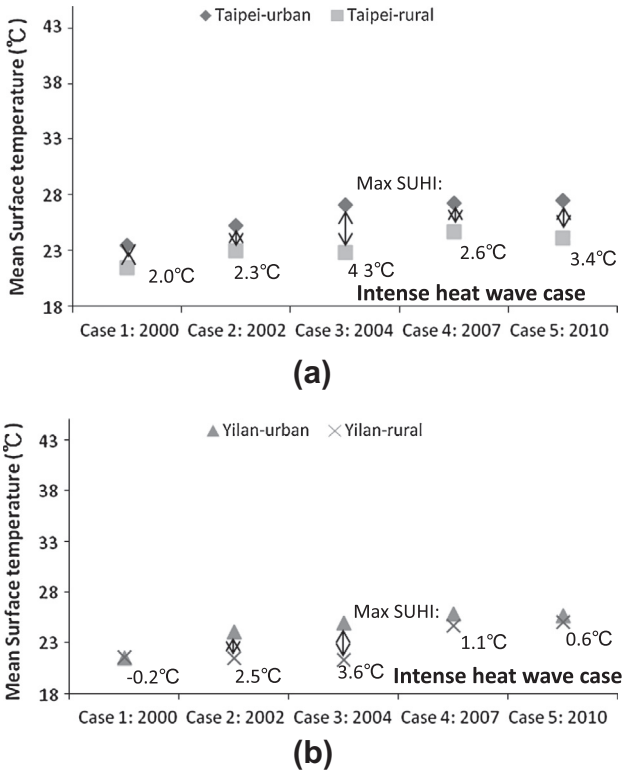


**Fig. 4.** Night time SUHI intensity (°C) of (a) Taipei metropolis and (b) Yilan area of the five selected heat wave cases.

obtained from DTMs have been validated and deemed reliable based on our previous work (Wu and Lung, 2012). Fig. 5 presents the calculated 3DUI maps of Taipei metropolis and Yilan area. It is anticipated that residential developments and human infrastructures are more extensive in Taipei than in Yilan. The highest 3DUI in Taipei and Yilan were 7714 and 2122 $m^3$/pixel, respectively. The estimated average 3DUI of Taipei (25 $m^3$/pixel) was about one order of magnitude higher compared with that of Yilan (3 $m^3$/pixel). The floor height of residential buildings in Taiwan is about 3.6 m (Ministry of the Interior, Republic of China, 2012b); thus, the results of 3DUI point out that on average there is a seven-floor building or construction in each 25 $m^2$ area of Taipei but only one single-floor building in the same area of Yilan.

Further to compare the 3DUI of the two urbanization types (urban and rural areas) in Taipei and Yilan, urban areas always had greater 3DUI values than rural areas in both Taipei (on average, urban: 229.4 $m^3$/pixel > rural: 1.1 $m^3$/pixel) and Yilan (on average, urban: 27.8 $m^3$/pixel > rural: 0.1 $m^3$/pixel), as expected. Comparing the two cities reveals that Taipei consistently had higher 3DUI values in both urbanization types. The largest difference with the value of 201.6 $m^3$/pixel was observed in the urban area. The value for the rural area of Yilan (0.1 $m^3$/pixel) was one order of magnitude smaller compared with that of Taipei (1.1 $m^3$/pixel). A small 3DUI value (0.1 $m^3$/pixel) indicates more vegetated areas or natural land covers in the countryside of Yilan area. On the other hand, urbanization has gradually expanded to the rural areas of Taipei; thus, 3DUI of 1.1 $m^3$/pixel was found in rural Taipei. Finally, examining the difference in urban–rural development between the two cities reveals that the urban–rural difference is greater in Taipei metropolis (228.3 $m^3$/pixel) than in Yilan (27.7 $m^3$/pixel). These results showed a significant difference in urbanization development between the core and periphery of Taipei metropolis; while urbanization development in Yilan was less abrupt between its city center and rural areas. The aforementioned comparison results are obviously consistent with difference in population density between the two cities, again demonstrating that the quantitative 3DUI is a good indicator of urbanization. The advantage of using 3DUI rather than other quantitative indicators, such as population density, is that 3DUI provides a much finer spatial resolution down to 5 m, thus allowing the SUHI to be examined in much finer resolution. This has important application and implications in identifying vulnerable areas under heat waves, which will be discussed below.

### 3.3.2. Correlation between 3DUI and surface temperature

In order to evaluate whether 3DUI is a good indicator for calculating SUHI intensity, the relationship between surface temperature and 3DUI was examined using the Spearman's rank order correlation. The size of pixel of the 3DUI maps was aggregated to 1 km × 1 km resolution based on a spatial mean aggregation strategy in order to be consistent with the LST images. In all the 10 adopted LST images, 41% of the study area was cloud-free (total 1204 $km^2$). Hence, they were adopted as samples for statistical comparison, and the results are listed in Table 3. As can be seen, all comparisons obtained positive correlations in the five cases (correlation coefficient >0.6 with statistically significant level $p < 0.01$). This result indicates that higher surface temperature occurs in the pixels with larger man-made construction volumes, in agreement with the expectation that more intensive urban development would have higher surface temperature. Therefore, 3DUI is proved to be a good indicator for evaluating the spatial variation of surface temperature and the intensity of SUHI. It can provide finer spatial variability of temperature compared with records of CWB stations and satellite images. 3DUI itself cannot provide absolute temperature values. However, combining 3DUI with tempera-

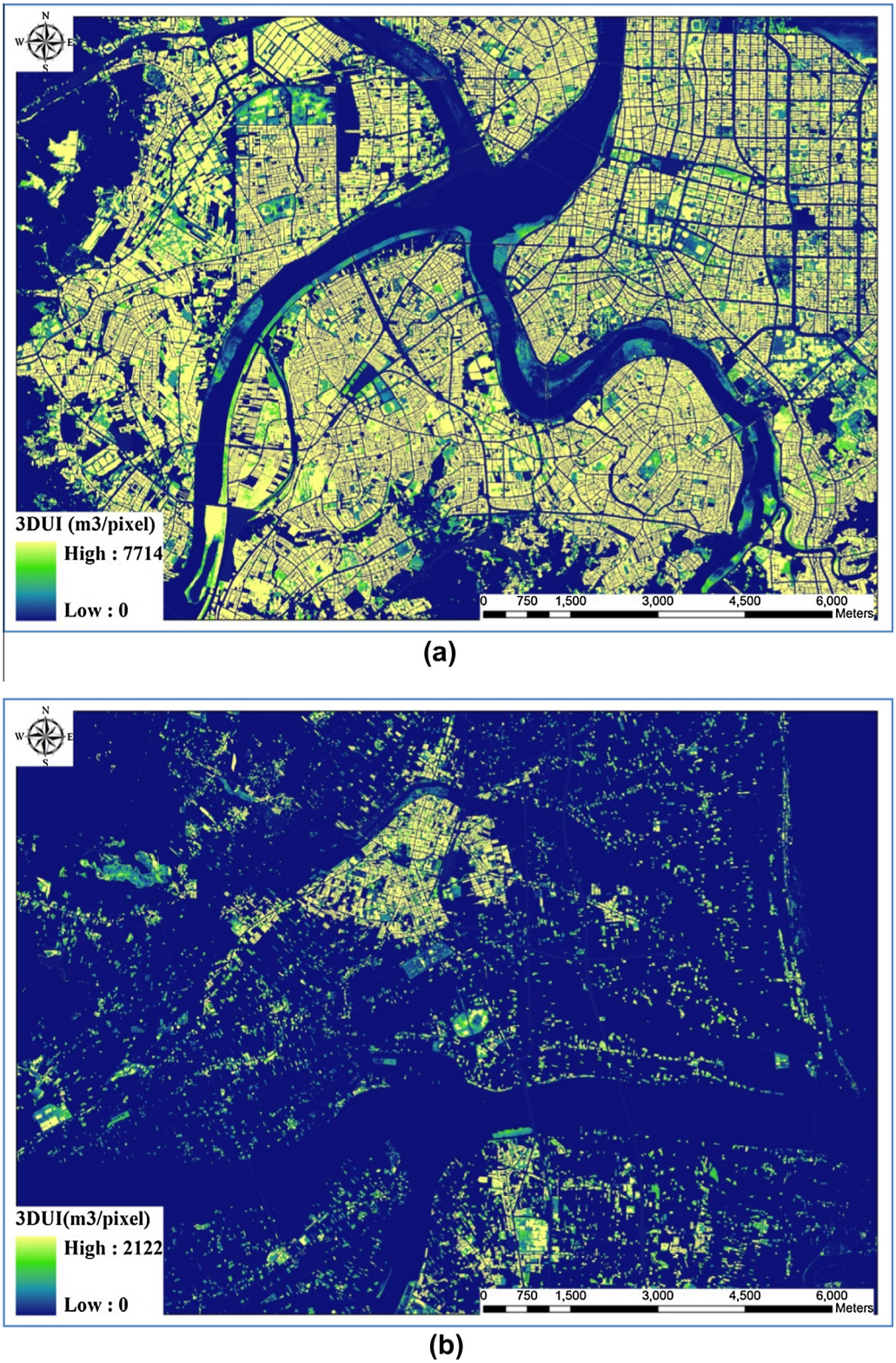


**Fig. 5.** 3DUI maps of part of the studied areas in (a) Taipei metropolis and (b) Yilan area; yellow in the maps indicates high construction volume while blue for non-construction areas with zero value. (For interpretation of the references to color in this figure legend, the reader is referred to the web version of this article.).

ture measurements from weather stations or from remote sensing yields finer spatial variation than the other two methods alone.

### 3.3.3. The potential application of 3DUI

The notions of people in subtropical areas being more adapted to hot weather and unaffected by heat waves are mistaken. Chung et al. (2009) examined the impact of heat waves on mortality in Taipei (1994–2003) and found that the respiratory mortality increased by 9.3% (confidence interval (C.I.) 4.1–14.8) per 1 °C increase when the air temperature rose above 31.5 °C; and cardiovascular mortality increased by 1.1% (C.I. 0.3–1.9) per 1 °C increase when the ground air temperature was above 25.2 °C. In

**Table 3**
Correlation coefficients between surface temperature (°C) and 3DUI ($m^3$/pixel), all comparisons are significant at 0.01 level ($p < 0.01$).

| | Sites | Correlation coefficient | | | | |
|---|---|---|---|---|---|---|
| | | Case 1 2000 | Case 2 2002 | Case 3 2004 | Case 4 2007 | Case 5 2010 |
| Daytime | Taipei + Yilan | 0.77[a] | 0.77 | 0.83 | 0.81 | 0.67 |
| | Taipei metropolis | 0.80 | 0.60 | 0.80 | 0.79 | 0.61 |
| | Yilan area | 0.67 | 0.66 | 0.70 | 0.65 | 0.67 |
| Night time | Taipei + Yilan | 0.64 | 0.71 | 0.80 | 0.66 | 0.70 |
| | Taipei metropolis | 0.60 | 0.64 | 0.77 | 0.63 | 0.72 |
| | Yilan area | 0.61 | 0.68 | 0.68 | 0.68 | 0.61 |

recent years, the air temperature in Taipei has frequently exceeded 35 °C, implying significant increases in respiratory and cardiovascular mortalities on hot days. Wu et al. (2010b) used temperature in Taipei above 35 °C as a cut-off point for defining heat waves and found that mortality significantly increased island wide during heat waves in 1994–2003 with evident spatial variability. To enhance adaptive capacity for heat waves, it is essential to identify vulnerable areas in fine spatial resolution in support of formulating heat wave adaptation strategies.

One of the important applications of 3DUI is for identification of vulnerable areas for heat waves. The relative spatial patterns of surface temperatures could be displayed by fine-resolution 3DUI ahead of heat waves since high correlation was found between 3DUI and surface temperature. The vulnerable population such as the elderly or children can be further identified by combining 3DUI with demographic database with age and sex distributions if available. The application would be particularly valuable for government administrators when formulating adaptation strategies to protect these vulnerable groups against heat stresses. In this study, a 5-m resolution was used because the datasets are available in Taiwan. Global DEM topographic data with 30-m resolution are available on the web (ASTER, 2012); thus, if DSM is available, 3DUI can be applied to other cities with 30-m resolution, which is sufficient for assessing temperature variation and SUHI intensity within a city.

This study is the first work applying GIS and DTMs to assess 3-D urbanization development with a 5-m spatial resolution. Our 3DUI methodology is an efficient way for assessing building height, which is an important factor of SUHI, over a large area. Compared with other 2-D urbanization indices such as the ratio of impervious surface, 3DUI provides a quantitative measurement of urbanization from a 3-D perspective. Besides, several image based indices have been proposed to assess SUHI, such as Normalized Difference Vegetation Index (NDVI), and Normalized Difference Built-up Index (NDBI), a spectrum based index for identifying urban and built-up areas (Zha et al., 2003). Yue et al. (2007) assessed the relation between NDVI and LST using Landsat Enhanced Thematic Mapper Plus (ETM+) images, their results showed that a $R^2$ value of 0.5 was observed after excluding pixels that correspond to water bodies; Li and Liu (2008) also stated low $R^2$ values (ranging from 0.06 to 0.3) were estimated between NDVI and MODIS surface temperature. Chen et al. (2006) show high correlation of LST and NDBI by intervals of 0.01 based on Landsat TM/ETM+ images ($R^2 = 0.98$, $p < 0.001$). However, the published results were not consistent. Xiong et al. (2012) presented a positive correlation with NDBI ($R^2 = 0.53$, $p < 0.001$) and a negative correlation with NDVI ($R^2 = 0.37$, $p < 0.001$) with LST based on four Landsat TM/ETM+ images with medium coefficients. In fact, both NDBI and NDVI only take into account two dimensional surface properties. The 3DUI we developed considers three dimensional urban structures; thus, 3DUI has a better correlation with MODIS LST than most of the reported in the literatures.

Image quality affects the applicability of remote sensing data on SUHI study. In Taiwan, it is not easy to acquire clear satellite images because of the cloudy and rainy weather conditions especially in summer (Wu et al., 2010b). Moreover, the resolution of thermal bands (e.g., 1-km resolution of bands 20–23 of MODIS) might not be suitable for analyzing the spatial variability of surface temperature over a small area. These factors limit the application of remote sensing indices to the identification of vulnerable area to heat stress. In this study, we proposed a fine-resolution 3DUI methodology as an alternative for investigating the relative spatial variation of temperature and SUHI. This methodology can be applied to other countries with available DTMs.

## 4. Conclusions

This study investigated the SUHI intensity during heat waves in Taipei metropolis (a large city) and Yilan area (a medium-sized city). The SUHI intensity in Taipei and Yilan can reach 10.2 and 7.5 °C during the five selected heat wave cases, respectively, which were higher than those on non-heat-wave days, indicating that SUHI intensity of both large and medium-sized cities were enhanced during heat waves. Comparing SUHI intensity in the two cities revealed that the difference can be as small as only 1.0 °C. Additionally, in the intense heat wave cases, the surface temperatures of rural areas in Taipei and Yilan were elevated, resulting in decreased SUHI intensity. One of the possible explanations is stomata closure mechanisms of vegetation under extremely high temperature conditions, which reduce the temperature regulation by vegetations. Thus, the SUHI may reach a plateau when the heat waves get stronger and last longer. As for the surface temperature of the five selected cases, the highest daytime temperature was up to 43.8 °C and 37.2 °C in urban Taipei and Yilan, respectively. Moreover, the elevated surface temperatures at night time of both Taipei and Yilan in the intense cases also indicated continuous thermal stress experienced by local residents even during the night. These results suggest that not only large cities but also medium-sized cities shall be taken into consideration when policy-makers formulate heat wave adaptation strategies.

Finally, this work presents an innovated 3DUI methodology to quantify 3-D urbanization development. It is an efficient method for estimating urbanization with a 5-m spatial resolution over a large area. From our experiments, all comparisons obtained positive correlations between 3DUI and surface temperatures (correlation coefficient >0.6 with $p < 0.01$). This result indicates that higher surface temperature occurs in the pixels with larger man-made construction volumes, in agreement with the expectation that more intensive urban development would have higher surface temperature. Thus, it can be employed to evaluate spatial variations of surface temperatures and SUHI intensity. Moreover, it can be utilized to identify vulnerable areas under heat waves in fine spatial resolution so that adaptation strategies can be formulated accordingly to reduce potential health risks of heat stress during heat waves with intensified SUHI.

## Acknowledgements

The authors acknowledge the grant supports from the Academia Sinica Thematic Project AS-101-SP-03 and the Research Center for Environmental Changes, Academia Sinica, Taiwan. We also thank the anonymous reviewers for their constructive comments on the early manuscript of the paper. Its contents are solely the responsibility of the authors and do not necessarily represent official views of funding agencies.

## References

Advanced Spaceborne Thermal Emission and Reflection Radiometer (ASTER), 2012. Global Digital Elevation Model 30m topographic data. <http://www.jspacesystems.or.jp/ersdac/GDEM/E/> (accessed 02.07.12).

Alagarni, D.A., El Hassan, I.M., 2001. Comparison of thin plate spline, polynomial, C1-function and Sheppard's interpolation techniques with GPS-derived DEM. International Journal of Applied Earth Observation and Geoinformation 3, 155–161.

Alonso, M.S., Labajo, J.L., Fidalgo, M.R., 2003. Characteristics of the urban heat island in the city of Salamanca, Spain. Atmósfera 16, 137–148.

Arnfield, A.J., 2003. Two decades of urban climate research: a review of turbulence, exchanges of energy and water, and the urban heat island. International Journal of Climatology 23 (1), 1–26.

Bottyán, Z., Kircsi, A., Szegedi, S., Unger, J., 2005. The relationship between built-up areas and the spatial development of the mean maximum urban heat island in Debrecen, Hungary. International Journal of Climatology 25, 405–418.

Braga, A.L., Zanobetti, A., Shwartz, J., 2001. The time course of weather-related deaths. Epidemiology 12, 662–667.

Brunn, A., Weidner, U., 1998. Hierarchical Bayesian nets for building extraction using dense digital surface models. ISPRS Journal of Photogrammetry and Remote Sensing 53, 296–307.

Chen, X.L., Zhao, H.M., Li, P.X., Yin, Z.Y., 2006. Remote sensing image-based analysis of the relationship between urban heat island and land use/cover changes. Remote Sensing of Environment 104 (3), 133–146.

Chung, J.Y., Honda, Y., Hong, Y.C., Pan, X.C., Guo, Y.L., Kim, H., 2009. Ambient temperature and mortality: an international study in four capital cities of East Asia. Science of the Total Environment 408 (2), 390–396.

Ciais, P., Reichstein, M., Viovy, N., Granier, A., Og ée, J., Allard, V., et al., 2005. Nature 437, 529–533.

Confalonieri, U., Menne, B., Akhtar, R., Ebi, K.L., Hauengue, M., Kovats, R.S., Revich, B., Woodward, A., 2007. In: Parry, M.L., Canziani, O.F., Palutikof, J.P., van der Linden, P.J., Hanson, C.E. (Eds.), Human Health. Climate Change 2007: Impacts, Adaptation and Vulnerability. Contribution of Working Group II to the Fourth Assessment Report of the Intergovernmental Panel on Climate Change. Cambridge University Press, Cambridge, UK, pp. 391–431.

Courault, D., Monestiez, P., 1999. Spatial interpolation of air temperature according to atmospheric circulation patterns in southeast France. International Journal of Climatology 19, 365–378.

Dessai, S., 2002. Heat stress and mortality in Lisbon. Part 1. Model construction and validation. International Journal of Biometeorology 47, 6–12.

Dessai, S., 2003. Heat stress and mortality in Lisbon. Part II. An assessment of the potential impacts of climate change. International Journal of Biometeorology 48, 37–44.

Directorate General of Budget (DGB), 2011. National Statistics-Current Index. <http://www.stat.gov.tw/point.asp?index=4> (accessed 07.06.12).

Donaldson, G.C., Keatinge, W.R., Näyhä, S., 2003. Changes in summer temperature and heat-related mortality since 1971 in North Carolina, South Finland, and Southeast England. Environmental Research 91, 1–7.

Forest Bureau, Republic of China, 2012. Vegetation Resources Inventory Using NDVI. <http://www.forest.gov.tw/content.asp?mp=112&Cultem=53041> (accessed 15.04.12).

Gallo, K.P., Owen, T.W., 1998. Assessment of urban heat islands: a multi sensor perspective for the Dallas Ft Worth, USA region. Geocarto International 13 (4), 35–41.

Gedzelman, S., Austin, S., Cermak, R., Stefano, N., 2003. Mesoscale aspects of the urban heat island around New York City. Theoretical & Applied Climatology 75, 29–42.

Gosling, S.N., McGregor, G.R., Páldy, A., 2007. Climate change and heat-related mortality in six cities, Part 1: model construction and validation. International Journal of Biometeorology 51, 525–540.

Hou, P.C., Tu, S.H., Liao, P.S., Hung, Y.T., Chang, Y.H., 2008. The typology of township in Taiwan: the analysis of sampling stratification of the 2005–2006 "Taiwan social change survey". Survey Research-Method and Application 23, 8–31.

Hung, T., Uchihama, D., Ochi, S., Yasuoka, Y., 2006. Assessment with satellite data of the urban heat island effects in Asian mega cities. International Journal of Applied Earth Observation and Geoinformation 8 (1), 34–48.

Huynen, M.M.T.E., Martens, P., Schram, D., Weijenberg, M.P., Kunst, A.E., 2001. The impact of heat waves and cold spells on mortality rates in the Dutch population. Environmental Health Perspectives 109, 463–470.

Kalkstein, L.S., Davis, R.E., 1989. Weather and human mortality: an evaluation of demographic and interregional responses in the United States. Annals of the Association of American Geographers 79, 44–64.

Kan, H., London, S.J., Chen, H., Song, G., Chen, G., Jiang, L., et al., 2007. Diurnal temperature range and daily mortality in Shanghai, China. Environmental Research 103, 424–431.

Kunzmann, R.K., 2009. Medium-sized Towns, Strategic Planning and Creative Governance, in the South Baltic Arc. <http://www.visible-cities.net/documents/KRK_MediumSized_Cities.pdf> (accessed 17.02.13).

Li, H., Liu, Q., 2008. Comparison of NDBI and NDVI as indicators of surface urban heat island effect in MODIS imagery. In: Li, D., Gong, J., Wu, H. (Eds.), International Conference on Earth Observation Data Processing and Analysis (ICEODPA). Proceedings of SPIE, pp. 728503-1–728503-10.

Liao, L.W., 2008. Application of MODIS Satellite Imagery Data to Estimate the Urban Heat Island Effect of the Metropolitan Cities in Taiwan. M.Sc. Thesis, Department of Forestry, National Pintung University of Science and Technology (in Chinese with English abstract).

Liu, Y.B., Hiyama, T., Yamaguchi, Y., 2006. Scaling of land surface temperature using satellite data: a case examination on ASTER and MODIS products over a heterogeneous terrain area. Remote Sensing of Environment 105 (2), 115–128.

Matinfar, H.R., Sarmadian, F., Alavi Panah, S.K., Heck, R.J., 2007. Comparisons of object-oriented and pixel-based classification of land use/land cover types based on Lansadsat7, ETM+ spectral bands-Case study: arid region of Iran. American–Eurasian Journal of Agricultural & Environmental Sciences 2 (4), 448–456.

Meehl, G.A., Tebaldi, C., 2004. More intense, more frequent and longer lasting heat waves in the 21st Century. Science 305 (5686), 994–997.

Meidner, H., Heath, O.V.S., 1959. Stomatal responses to temperature and carbon dioxide concentration in *Allium cepa* L. and their relevance to midday closure. Journal of Experimental Botany 10 (2), 206–219.

Ministry of the Interior, Republic of China, 2011. Regulations of Urban Road Designs. <http://myway.cpami.gov.tw/way/sites/default/files/shi_qu_dao_lu_ji_fu_shu_gong_cheng_she_ji_gui_fan_9804_2.pdf> (accessed 07.06.12).

Minister of the Interior, Republic of China, 2012a. National GIS Socio-economic Data Warehouse. <http://segis.moi.gov.tw/> (accessed 04.03.12).

Ministry of the Interior, Republic of China, 2012b. Rules of Architecture Techniques. <http://glrs.moi.gov.tw/LawContentDetails.aspx> (accessed 04.08.12).

National Land Surveying and Mapping Center (NLSMC), 2009. Land Use Investigation of Taiwan. <http://lui.nlsc.gov.tw/LUWeb/eng/AboutLU.aspx> (accessed 15.07.12).

Oke, T.R., 1973. City size and the urban heat island. Atmospheric Environment 7 (8), 769–779.

Oke, T.R., 1982. The energetic basis of the urban heat island. Quarterly Journal of the Royal Meteorological Society 108 (455), 1–24.

Oke, T.R., Johnson, G.T., Steyn, D.G., Watson, I.D., 1991. Simulation of surface urban heat islands under 'ideal' conditions at night. Part 2: diagnosis of causation. Boundary-Layer Meteorology 56 (4), 339–358.

Páldy, A., Bobvos, J., Vámos, A., Kovats, R.S., Hajat, S., 2005. The effect of temperature and heat waves on daily mortality in Budapest, Hungary, 1970–2000. In: Kirch, W., Menne, B., Bertollini, R. (Eds.), Extreme Weather Events and Public Health Responses. Springer, Berlin, pp. 99–107.

Papanastasiou, D.K., Kittas, C., 2012. Maximum urban heat island intensity in a medium-sized coastal Mediterranean city. Theoretical and Applied Climatology 107 (3–4), 407–416.

Pattenden, S., Nikiforov, B., Armstrong, B.J., 2003. Mortality and temperature in Sofia and London. Journal of Epidemiology and Community Health 57, 628–633.

Pongracz, R., Bartholy, J., Dezso, Z., 2006. Remotely sensed thermal information applied to urban climate analysis. Advances in Space Research 37 (12), 2191–2196.

Rondinelli, D.A., 1993. Secondary Cities in Developing Countries: Policies for Diffusing Urbanization. Sage, Beverly Hills.

Saez, M., Sunyer, J., Tobias, A., Ballester, F., Antó, J.M., 2000. Ischaemic heart disease and weather temperature in Barcelona, Spain. The European Journal of Public Health 10, 58–63.

Satellite Survey Center (SSC), 2011. High Precision and High Resolution DTM. <http://www.gps.moi.gov.tw/sscenter/> (accessed 12.12.12).

Schroeder, J.I., Kwak, J.M., Allen, G.J., 2001. Guard cell abscisic acid signalling and engineering drought hardiness in plants. Nature 410, 327–330.

Sheriff, D.W., 1979. Stomatal aperture and the sensing of the environment by guard cells. Plant, Cell & Environment 2 (1), 15–22.

Smoyer-Tomic, K.E., Kuhn, R., Hudson, A., 2003. Heat wave hazards: an overview of heat wave impacts in Canada. Natural Hazards 28 (2–3), 465–486.

Solomon, S., Qin, D., Manning, M., Chen, Z., Marquis, M., Averyt, K.B., Tignor, M., Miller, H.L., 2007. Climate Change 2007: The Physical Science Basis. Cambridge University Press, Cambridge, United Kingdom and New York, NY, USA, 996 pp.

Stathopoulou, M., Cartalis, C., 2007. Daytime urban heat islands from Landsat ETM+ and Corine land cover data: an application to major cities in Greece. Solar Energy 81 (3), 358–368.

Streutker, D.R., 2003. Satellite-measured growth of the urban heat island of Houston, Texas. Remote Sensing of Environment 85, 282–289.

Tan, J., Zheng, Y., Tang, X., Guo, C., Li, L., Song, G., et al., 2010. The urban heat island and its impact on heat waves and human health in Shanghai. International Journal of Biometeorology 54 (1), 75–84.

Tomlinson, C.J., Chapman, L., Thornes, J.E., Baker, C.J., 2012. Derivation of Birmingham's summer surface urban heat island from MODIS satellite images. International Journal of Climatology 32, 214–224.
Unger, J., Savic, S., Gail, T., 2011. Modelling of the Annual Mean Urban Heat Island Pattern for Planning of Representative Urban Climate Station Network. Advances in Meteorology, 9. http://dx.doi.org/10.1155/2011/398613.
United Nations, 2008. Population Division of the Department of Economic and Social Affairs of the United Nations Secretariat, Population Prospects: The 2008 Revision Highlights. United Nations, New York.
United Nations Children's Fund (UNICEF), 2012. An Urban World. <http://www.unicef.org/sowc2012/urbanmap/> (accessed 23.10.12).
United State Census Bureau, 2013. Metropolitan Statistical Area. <http://quickfacts.census.gov/qfd/meta/long_metro.htm> (accessed 17.02.13).
United State Geological Survey (USGS), 2011. Rocky Mountain Mapping Center. <http://rockyweb.cr.usgs.gov/elevation/dpi_dem.html> (accessed 22.05.12).
Voogt, J.A., Oke, T.R., 2003. Thermal remote sensing of urban climates. Remote Sensing of Environment 86 (3), 370–384.
Wan, Z., 2009. Collection-5 MODIS Land Surface Temperature Products Users' Guide. ICESS, University of California, Santa Barbara.
Watkins, R., Palmer, J., Kolokotroni, M., 2002. The London heat island: results from summertime monitoring. Building Services Engineering Research and Technology 23 (2), 97–106.
Weng, Q., Lu, D., Schubring, J., 2004. Estimation of land-surface temperature-vegetation abundance relationship for urban heat island studies. Remote Sensing of Environment 89, 467–483.
World Health Organization (WHO), 2009. Improving Public Health Responses to Extreme Weather/Heat-Waves: EuroHEAT, Technical Summary. <http://www.euro.who.int/__data/assets/pdf_file/0010/95914/E92474.pdf> (accessed 01.03.12).
Wu, C.D., Cheng, C.C., Lo, H.C., Chen, Y.K., 2010a. Study on estimating the evapotranspiration cover coefficient for stream flow simulation through remote sensing techniques. International Journal of Applied Earth Observation and Geoinformation 12 (4), 225–232.
Wu, C.D., Lung, C.C.C., 2012. Applying GIS and fine-resolution digital terrain models to assess three-dimensional population distribution under traffic impacts. Journal of Exposure Science and Environmental Epidemiology 22 (2), 126–134.
Wu, P.C., Lin, C.Y., Lung, S.C.C., Guo, H.R., Chou, C.H., Su, H.J., 2010b. Cardiovascular mortality during heat and cold events: determinants of regional vulnerability in Taiwan. Occupational Environmental Medicine. http://dx.doi.org/10.1136/oem.2010.056168.
Xiong, Y., Huang, S., Chen, F., Ye, H., Wang, C., Zhu, C., 2012. The impacts of rapid urbanization on the thermal environment: a remote sensing study of Guangzhou, South China. Remote Sensing 4, 2033–2056.
Yow, D.M., 2007. Urban heat islands: observations, impacts, and adaptation. Geography Compass 1 (6), 1227–1251.
Yue, W., Xu, J., Tan, W., Xu, L., 2007. The relationship between land surface temperature and NDVI with remote sensing: application to Shanghai Landsat 7 ETM+ data. International Journal of Remote Sensing 28 (15), 3205–3226.
Zha, Y., Gao, J., Ni, S., 2003. Use of normalized difference built-up index in automatically mapping urban areas from TM imagery. International Journal of Remote Sensing 24 (3), 583–594.